FRACTURE TOUGHNESS OF LOW TEMPERATURE CARBON STEEL FLANGES

E. Blakeley* and P. Bowen*

This paper reports on the fracture toughness of large carbon steel flanges for use offshore at service temperatures of -64°C and above. Such large scale forgings are often difficult to heat-treat adequately and are found to possess extremely poor toughness particularly if Widmannstatten ferrite is present. Micromodelling of fracture toughness behaviour indicates that flanges heat-treated correctly after forging cannot fail by cleavage fracture at envisaged service temperatures, whereas incorrectly or non heat-treated forgings may be susceptible to cleavage even at ambient temperature. The paper links macroscopic toughness with microstructure for as-received full-size forgings.

INTRODUCTION

Several recent studies have found large steel flanges (for use in pipelines of up to 1100 mm diameter) to possess poor toughness. Problems may arise when accompanying test-certification is based on smaller-scale test bars supplied from the same heat of material (as is common practice), since they are unlikely to represent accurately the forging and heat-treatment schedules performed subsequently to produce the final flanges. This study is based on full size flanges order to ASTM specification A350 LF2 (which requires 20 Joules at -46.5°C) and made available following a retest programme. Maximum compositional limits (wt.%) allowable under the specification are 0.3 C, 0.3 Si, 1.35 Mn, 0.035 P, 0.04 S. In the prior study from a sample of 44 flanges, all with adequate test certification, 16 flanges failed on testing impact specimens machined from the finished flanges. A detailed fitness-for-purpose assessment has since been performed, see Bowen et al. (1), when worst case operating conditions at -64°C were assumed (for gas-plant piping systems this is the lowest temperature that can be reached on theoretical grounds (1)). This work investigates the micromechanisms of failure of such full-size flanges, and attempts to predict safe operating temperatures in service.

*School of Metallurgy and Materials/IRC in Materials for High Performance Applications, University of Birmingham.

EXPERIMENTAL

Material was selected based on previous impact tests at -50°C, see Table 1. A comprehensive series of Fracture Toughness tests (SEN bend testpieces W = B = 20 mm), blunt-notch tests (see Griffiths and Owen (2)) and tensile tests (Hounsfield No. 13) were performed at temperatures from -196 to + 20°C.

Blunt notch testing was used to establish the maximum value of local tensile stress (σ_F*) present at fracture (also termed the microscopic cleavage fracture stress). Fracture toughness was performed in accordance with BS5762: 1979 (3). In addition detailed fractography and optical metallography was carried out.

RESULTS

Tensile strengths and 0.2% proof stresses are shown versus test temperature in Figure 1. No significant differences are observed between the flange materials under investigation. The work hardening exponent, n, calculated from true stress-true strain measurements made at -120°C, is equal to 0.20 for both flange materials. Reduction in area measurements are also shown in the Figure, and indicate for both conditions values in excess of 60% at temperatures of -80°C and above.

Crack opening displacement values are shown versus test temperature in Figure 2. Flange material 70405 possesses markedly reduced toughness and an estimated sharp-crack transition region approximately 100°C higher compared with flange material 70365. Indeed, maximum load crack opening displacement, δ_m, values of 0.60 mm are obtained at -70°C for flange material 70365 whereas unstable (cleavage) crack opening displacement, δ_u, values (3) of 0.06 mm are obtained at +20°C for flange material 70405. Values of the microscopic cleavage fracture stress, σ_F*, calculated from blunt-notch tests are 2100 and 1470 MPa for flange materials 70365 and 70405 respectively. These values were obtained from failure loads at -196°C - the only temperature at which the ratio of $\sigma_{nom}/\sigma_{0.2}$ (where σ_{nom} is defined as the nominal bending stress on the notched cross-section, and $\sigma_{0.2}$ is the 0.2% proof stress) was before general yielding and within the range of the Griffiths and Owen finite element analysis (2).

TABLE 1 - Materials selected for present study based on previous retest programme

Flange number	Test Temperature (°C)	Impact Energy C_v (Joules)
70365	-50	168, 175, 255
70405	-50	5, 6, 8

Values of fracture toughness are given in Figure 3. A valid fracture toughness, K_{IC}, was obtained at -196°C, but at all other test temperatures specimen size requirements (4) were violated and only K_Q values were obtained. For flange material 70365 tested at -70°C the value of toughness shown has been calculated from the maximum load observed on the load-clip gauge displacement curve. Also shown in Figure 3 are the predictions of the fracture toughness with test temperature made using the RKR model (5), Bowen et al. (6). This assumes both a value of σ_F* and characteristic distance, X_o to be independent of test temperature. Failure is predicted to occur when values of local stress ≥ σ_F* are exceeded over the characteristic distance, X_o. This distance cannot be related in general to any microstructural parameter, but it can be evaluated using the local stresses ahead of a sharp crack, Figure 4, by fitting data at a temperature for which K_{IC} (or K_Q) is known. X_o is calculated as 51.5 and 50.0 μm for the flange materials 70365 and 70405 respectively. The upward trend in toughness can then be predicted from the temperature variation of the proof stress using Figure 4 if the value of the work hardening exponent, n is known.

Optical micrographs are shown in Figures 5 and 6 for the flange materials 70365 and 70405 respectively. Clearly the latter material contains coarser ferrite grains and evidence of Widmannstatten ferrite. The mean ferrite grain size is 28.7 ± 13.2 μm, prior austenite grain size of 110.2 ± 42 μm, and length and width of the Widmanstatten plates 20.6 ± 12.2 and 11.9 ± 6.6 μm respectively. Flange material 70365 has a ferrite grain size of 13.1 ± 6.1 μm, and contains colonies of fine pearlite. Grain boundary carbides were observed with difficulty for both flange materials with a mean size of 0.2 ± 0.07 μm. The coarsest observed carbide thickness was 0.39 and 0.50 μm for the flange materials 70365 and 70405 respectively. Despite careful fractographic observations and microanalysis no fracture initiation sites could be identified rigorously. The mean facet size was 26 ± 9 and 55 ± 16 μm for the flange materials 70365 and 70405 respectively. Clearly the larger cleavage facets are easier to observe, since there should be a direct one-to-one correlation with the ferrite grain size.

DISCUSSION

Flange material 70405 does not appear to have been normalised subsequent to forging, as evidenced by its coarse microstructure and the presence of Widmanstatten ferrite, Figure 6. This is in sharp contrast to flange material 70365. Both materials however, have satisfactory tensile properties at envisaged service temperatures, indicating the vital role of fracture toughness testing in defect tolerance assessment. The importance of σ_F* in assessing cleavage fracture resistance is apparent and in this study its interpretation for the two microstructures is made easy by their closely similar yield stresses at all temperatures.

Indeed, since the maximum possible stress intensification from Figure 3 is $\sigma_{11}/\sigma_{0.2} = 5.10$ where σ_{11} is the maximum value of local tensile stress, then it is predicted that cleavage fracture cannot occur (i.e. $\sigma_{11} = \sigma_F$*) when the 0.2% proof stress is less than 412 and 290 MPa for flange materials 70365 and

70405respectively. Therefore the upper temperatures for cleavage are predicted to be -80 and >20°C for the flange materials 70365 and 70405 respectively, consistent with the experimental observations.

The large differences in σ_F* measured for the two materials cannot be explained by the small difference in coarsest observed carbide sizes (through a modified Griffith criterion) and indicates strongly the influence of grain size and/or the presence of Widmanstatten ferrite plates on cleavage fracture. Such effects still cannot be accounted for satisfactorily in present day models and highlight the difficulties inherent to producing a quantitative statistical analysis of cleavage fracture. Although in many instances (6) the RKR model fails to predict observed trends with temperature adequately, in the present study it provides a consistent qualitative picture, Figure 4, and distinguishes clearly between the two materials. In general, this model appears to work more satisfactorily when the material has a high work hardening exponent, n, equal to 0.2. In the present example reasonable agreement is found if the characteristic distance is equated to twice the ferrite grain size as in the original paper (5), but this is regarded as fortuitous. This present work indicates the usefulness of micromechanistic parameters in rationalising macroscopic toughness in engineering situations.

CONCLUSIONS

Marked differences in toughness have been observed to occur as a result of incorrect heat-treatment of large size flanges. Coarse ferrite grains and Widmanstatten ferrite reduce the toughness dramatically. Correctly heat-treated forgings cannot fail by cleavage at envisaged in-service temperatures. Macroscopic engineering toughness has been predicted qualitatively using micromechanistic models of cleavage fracture.

ACKNOWLEDGEMENTS

The authors would like to thank Shell Research Ltd. for the provision of material, and Dr. R.A. Bartlett for helpful discussions.

REFERENCES

1. Bowen, P., Frost, S.R. and Bartlett, R.A., submitted for publication to Int. Journ. Press. Vess. and Piping, April 1990.
2. Griffiths, J.R. and Owen, D.R.G., J. Mech. Phys. Sol., Vol. 21, 1971, pp. 419-431.
3. BS 5762: 1979 Methods for crack opening displacement (COD) testing.
4. BS 5447: 1977 Methods for plane strain fracture toughness testing of metallic materials.
5. Ritchie, R.O., Knott, J.F. and Rice, J.R., J. Mech. Phys. Sol., Vol. 21, 1973, pp. 395-405.
6. Bowen, P., Druce, S.G. and Knott, J.F., Acta Metall. Vol. 35, No. 7, 1987, pp. 1735-1746.

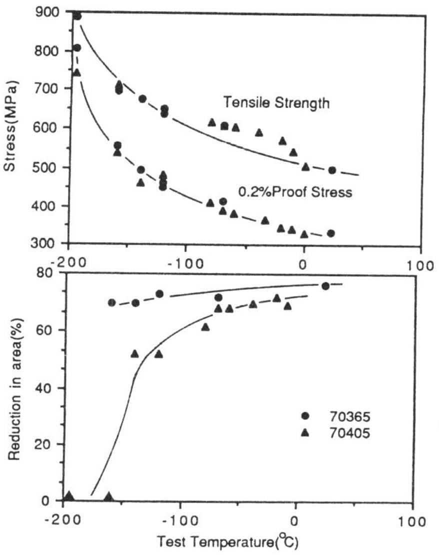

Figure 1 Tensile Properties versus test temperature

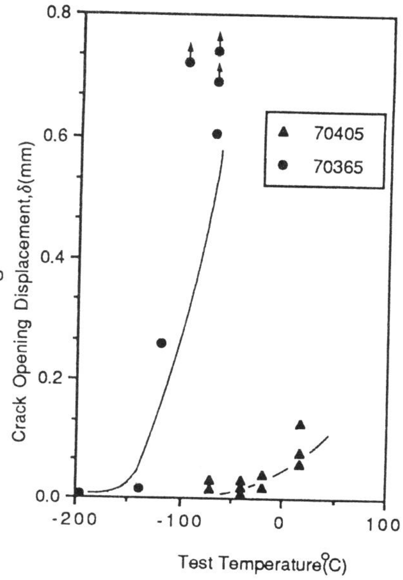

Figure 2 Crack opening displacement versus test temperature

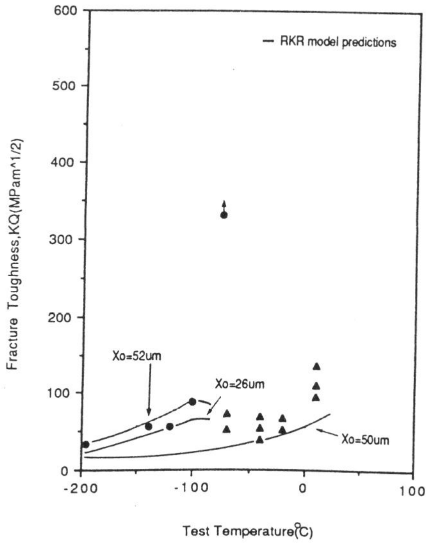

Figure 3 Fracture toughness, K_Q, versus test temperature

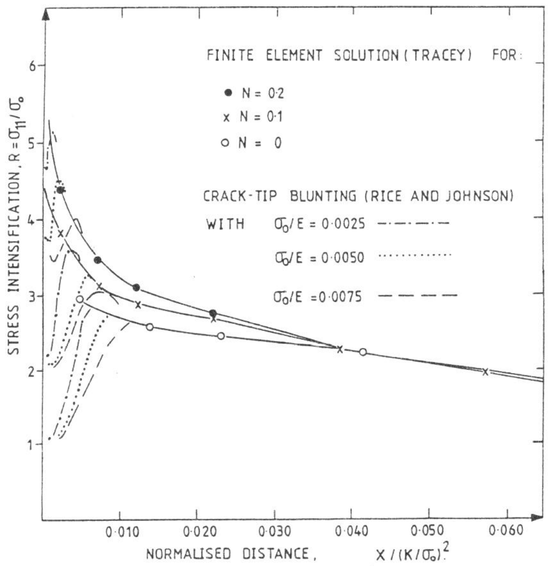

Figure 4 Maximum tensile stress, σ_{11}, ahead of crack-tip.

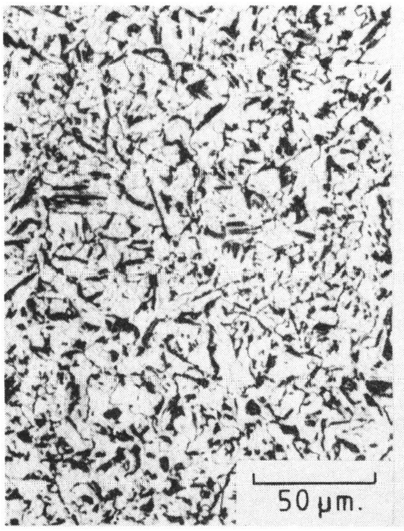

Figure 5 Optical micrograph of flange material 70365

Figure 6 Optical micrograph of flange material 70405